Zitierweise: *Angew. Chem. Int. Ed.* **2022,** *61,* e202116324
Internationale Ausgabe: doi.org/10.1002/anie.202116324
Deutsche Ausgabe: doi.org/10.1002/ange.202116324

DNA Origami

Spatiotemporal Control of Molecular Cascade Reactions by a Reconfigurable DNA Origami Domino Array

*Sisi Fan, Bin Ji, Yan Liu, Kexuan Zou, Zhijin Tian, Bin Dai, Daxiang Cui, Pengfei Zhang, Yonggang Ke, and Jie Song**

Abstract: *Inspired by efficient biomolecular reactions in the cell, versatile DNA nanostructures have been explored for manipulating the spatial position and regulating reactions at the molecular level. Spatially controlled arrangement of molecules on the artificial scaffolds generally leads to enhanced reaction activities. Especially, the rich toolset of dynamic DNA nanostructures provides a potential route towards more sophisticated and vigorous regulation of molecular reactions. Herein, a reconfigurable DNA origami domino array (DODA) as a dynamic scaffold was adopted in this work for temporal-controlled and switchable molecular cascade reactions. Dynamic regulation of the assembly of G-quadruplex, hybridization of parallel-stranded duplex and assembly of binary DNAzyme were demonstrated. Molecular cascade reactions on the triggered reconfiguration of DODAs were realized, resulting in more complex, dynamic, and switchable control over the reactions.*

Introduction

Cascade reactions, in which several reactions occur in a sequential manner in the same reaction apparatus, are chemically very efficient and could quickly build up the molecular complexity. In biological systems, cascade reactions generally occur under conditions that are constant overall and are regulated by spatially confined molecular mechanisms.[1] Despite many advances,[2] it is still a formidable challenge to reconstitute and reprogram the reactions which process similar complexity as the natural biological systems in the laboratory. Extensive efforts have been directed to develop organized systems and mimic such spatially confined biological cascade reactions in vitro. One of the emerging methodologies is to utilize DNA nanotechnology in spatially controlled reaction systems.

DNA nanotechnology has contributed major breakthroughs toward programmable and nanoscale assembly, localization, and organization.[3] Various self-assembled DNA nanostructures[4] have served as organized reaction scaffolds and vessels, resulting in the artificially templated cascade platforms. For example, single-molecular chemical reactions have been conducted in DNA origami.[5] Proximity-induced activation and inhibition of multiple intrinsically associating signaling components (e.g. caspase-9) have been demonstrated on a DNA origami-based synthetic apoptosome.[6] Investigations of enzymatic cascades have been realized by scaffolding multiple enzymes in the DNA nanostructures.[7] However, the majority of reported DNA-scaffolded cascades still encounter the limitation of simultaneous control over the time-dependent positioning of the scaffolded components. Building upon the principle of strand displacement reaction, dynamic DNA nanotechnology[8] in the form of DNA walkers[9] provided autonomous multistep organic reactions,[10] proximity-induced pattern operations,[4c] and control of enzyme reactions,[4e] etc. Though promising, it is still crucial to develop systems that can provide both spatial and temporal control over cascade reactions, imitating the complex dynamics of natural systems within the laboratory.

Herein, we present a dynamic platform to accommodate molecular cascade reactions under a temporal-controlled, switchable operation based on the reconfigurable DODA nanostructures reported by our group previously,[8c,d,11] which can dynamically transform among four different conformations. The DODA nanostructure was used to spatially organize the reactants A and B, and further guide and assist A and B to form products C in a controlled manner. (Figure 1A). In the free system, the reactants A and B can diffuse and collide randomly, and further react with each other. The reaction process of A and B is influenced by the reactants' concentration and temperature, etc. These factors essentially move the equilibrium of the reaction from one to the other side, leading to mainly three types of reactions (termed as "side" reaction, reversible reaction and "inert" reaction). For the "side" reaction, A

[*] Dr. S. Fan, Dr. B. Ji, Y. Liu, K. Zou, Prof. B. Dai, Prof. D. Cui, Prof. J. Song
Institute of Nano Biomedicine and Engineering
Department of Instrument Science and Engineering
School of Electronic Information and Electrical Engineering
Shanghai Jiao Tong University, Shanghai 200240 (China)
E-mail: sjie@sjtu.edu.cn
Z. Tian
Department of Chemistry
University of Science & Technology of China
230026, Anhui, Hefei, (China)
Prof. Y. Ke
Wallace H. Coulter Department of Biomedical Engineering
Georgia Institute of Technology and Emory University
Atlanta, GA 30322 (USA)
Z. Tian, P. Zhang, Prof. J. Song
Institute of Cancer and Basic Medicine (IBMC)
Chinese Academy of Sciences
The Cancer Hospital of the University of Chinese Academy of Sciences
310022, Zhejiang, Hangzhou, (China)

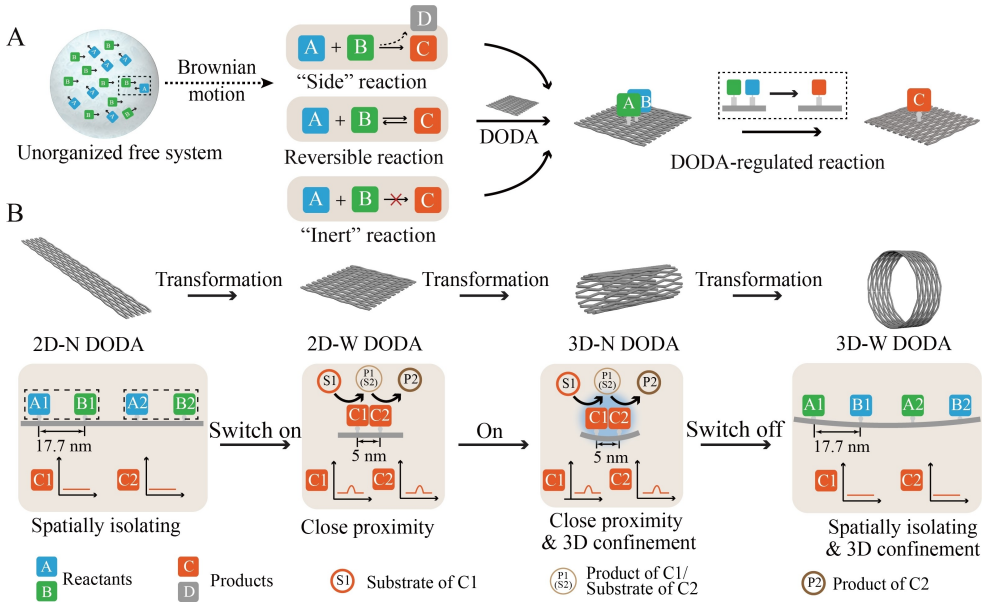

Figure 1. Engineering molecular cascade reactions in reconfigurable DODA. A) DODA nanostructure was used to regulate three types of reactions, termed as "Side" reaction, reversible reaction and "Inert" reaction in a free system. B) Organizing and programming products C with four different array configurations in the four DODAs (top). Note that, the "1D array, 2D array, 3D-N array and 3D-W array" represented by the products C were programmed as the specific arrays in the 2D-N, 2D-W, 3D-N and 3D-W DODAs, respectively. Molecular cascade reactions were dynamically controlled and regulated by the transformation of DODAs from 2D-N to 2D-W, then to 3D-N, final to 3D-W (down). Reconfiguration of the 2D-N DODA to 2D-W DODA brought A1 close to B1, A2 close to B2. C1 was formed by its sub-units of A1 and B2. C2 was formed by its sub-units of A2 and B2 in the 2D-W DODA. If the B1 and A2 were designed as distinct sub-units of other products (e.g. C3), the reconfiguration of the 2D-N DODA to 2D-W DODA could also bring B1 close to A2 to form C3. The inserted graphs next to C1 and C2 illustrated the formation of C1 and C2. The peak was used to indicate the formation of the product. When in 2D-N DODA, A1 and B1, A2 and B2 were spatially isolated, C1 and C2 could not be formed. There were no corresponding peaks. Then the transformation of the DODA from 2D-N to 2D-W could bring A1 close to B1, A2 close to B2, leading to the formation of C1 and C2.

reacts with B to form C, as well as the by-products D. For the reversible reaction, the reaction process of A and B is reversible. For the "inert" reaction, A is difficult to react with B to form C. Versatile DODA could further reconfigure from 2D-narrow (2D-N) to 2D-wide (2D-W), 3D-narrow (3D-N), and 3D-wide (3D-W) conformations with distinct trigger strands (Figure 1B). The conformational transformation not only regulates the reactants into proximity by self-assembly reactions, but also spatially isolates the reactants to disassemble. Additionally, triggered reconfiguration of DODAs further provided complex, dynamic, and switchable control over the molecular cascade reactions.

Results and Discussion

DODA Regulated Assembly of G-Quadruplex

For the "side" reaction, in the free system, reactants A and B with reactive groups can react with each other to form C easily. Meanwhile, some byproducts could also be generated (Figure 2A). Taking the assembly of G-quadruplex as an example (Figure 2B and S3), in the presence of K^+, G1 and G2 could assemble into G-quadruplex, while G2 and G2 could also assemble into another G-quadruplex (side product). In the presence of hemin, the formed hemin/G-quadruplex horseradish peroxidase-mimicking DNAzyme further performed catalytic activities towards the H_2O_2-mediated oxidation of 3,3′,5,5′-tetramethylbenzidine (TMB), resulting in a colored product. The generation of byproducts by two G2 was confirmed by gel-electrophoresis analysis (Figure S4). The UV/Vis absorption spectroscopy further verified that the byproducts were formed from two G2 units (Figure 2D, orange curve). To regulate the assembling of G1 and G2 rather than two G2 units into the desired G-quadruplex, a controlled reaction system using a rectangular DODA (named as 2D-W DODA, Figure S5–S7) was constructed. As shown in Figure S8, five Blocked-G1 and Blocked-G2 units were tightly positioned. In this case, the distance between Blocked-G1 and Blocked-G2 was about 5 nm, which was reachable for activated G1 and G2 to assemble into G-quadruplexes. The absorbance at 650 nm indicated the formation of G-quadruplexes in 2D-W DODA nanostructure (purple line in Figure 2D). Notably, when programming G1 and G2 in the 2D-W DODA, G1 and G2 were blocked prior to prevent the non-specific reactions (see the Methods parts of "Assembling G-quadruplex in DODA" in the Supporting Information). If not, the excess G1 /G2 could assemble with the activated G2/G1 in the 2D-W DODA. After blocking the G1 and G2 in the 2D-W DODA (Figure 2D, blue curve), the non-specifical G-quadruplex did not form. After activation of the Blocked-G1 and Blocked-G2, the G1 and G2 formed a single G-quadruplex in 2D-W DODA (Figure 2D, purple curve).

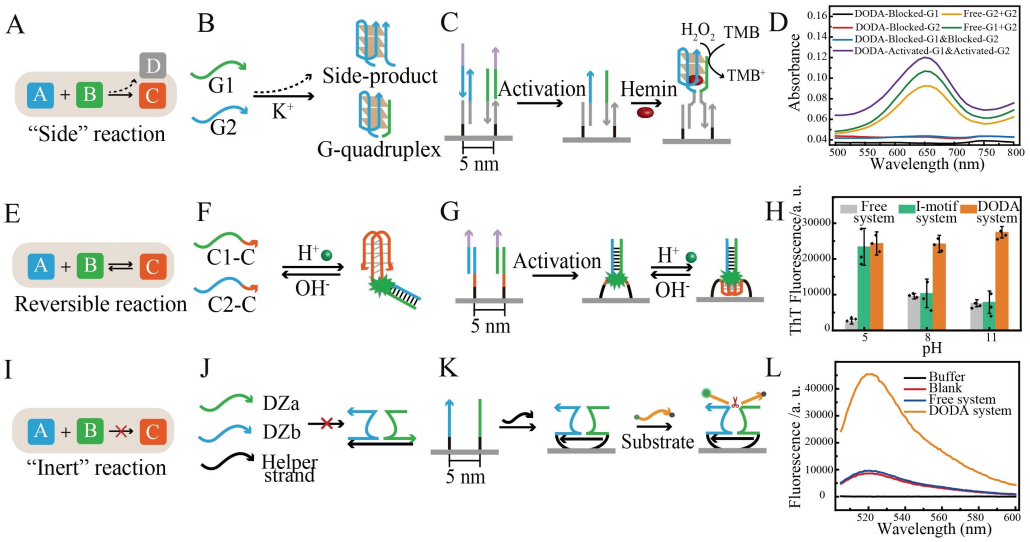

Figure 2. Molecular reactions in the free system and DODA system. A) For the side reaction, A reacts with B to form C, as well as the byproducts of D. B) Assembly of G-quadruplex in 2D-W DODA in the free system. Taking the G1 and G2 to form G-quadruplex as an example, in the free system, G1 and G2 assemble into G-quadruplex. G2 and G2 assemble into another G-quadruplex (side-product). C) Assembly of G-quadruplex in the 2D-W DODA nanostructure. D) UV/Vis absorption spectra of the formed G-quadruplex in the free system and DODA system. E) For the reversible reaction, A reacts with B to form C in a specific condition, and then disassembles in another condition in the free system. In the systems of Free-G2+G2 (orange line), Free-G1+G2 (green line) and DODA-Activated-G1& Activated-G2 (purple line), the formed G-quadruplexes performed catalytic activities towards the H_2O_2-mediated oxidation of TMB to produce theTMB$^+$, resulting in the new absorption peak at 650 nm. In the systems of DODA-Blocked-G1 (black line), DODA-Blocked-G2 (red line) and DODA-Blocked-G1 & Blocked-G2 (blue line), there were no G-quadruplexes formed. The TMB could not be oxidized, resulting in no absorption peak at 650 nm. F) Hybridization of the parallel-stranded duplex was regulated by the i-motif DNA nanostructure. When in acidic medium, the hybridization of parallel-stranded duplex was enhanced due to the formation of the i-motif between the C traits of the C1-C and C2-C sequences. The disassemble of the i-motif then separated the parallel-stranded duplex in alkaline medium. G) Hybridization of the parallel-stranded duplex in the 2D-W DODA nanostructure. H) Comparisons of the hybridization degree of parallel-stranded duplex in the free system, i-motif system, and 2D-W DODA system with different pH values. Note that for the free system: C1 and C2 are in solution; for the i-motif system: C1-C and C2-C are in solution; and that for the DODA system: C1-C and C2-C programmed in DODA in solution. I) For the "Inert" reaction, A cannot react with B to form C. J) Taking the assembly of binary DNAzyme (assembly of DZa, DZb and Helper strand) as an example, in the free system, DZa, DZb and Helper strand cannot assemble into the DNAzyme, or then cleave the substrate. K) Assembly of binary DNAzyme in the 2D-W DODA nanostructure. L) Fluorescence spectra of the cleavage of substrate in the free and DODA system.

Additionally, further support for the formation of G-quadruplexes in 2D-W DODA was confirmed by fluorescence resonance energy transfer (FRET) experiments. The G2 was modified by Atto488, and the G1 was modified by BHQ1 (Atto 488 was quenched by BHQ1). The FRET effect was observed upon the formation G-quadruplexes in DODA nanostructures (see Figure S11 and corresponding discussion).

Since the assembly of G-quadruplex is involved in the dimerization, it is envisioned that the reaction could be tuned by varying the distance between the monomers of G1 and G2. To this end, the distances between G1 and G2 were varied from 5.0, 10.0, 17.7, 35.4 to 70.8 nm, followed by exploring the catalytic activities of the formed G-quadruplexes. The highest catalytic activities were observed when the monomers were in close proximity (<10.0 nm), after which the activities dropped sharply and approached background activity levels when separating (>10 nm), indicating assembly of G-quadruplex at the pre-programmed positions (Figure S12 and Figure S13).

DODA Regulated Hybridization of the Parallel-Stranded Duplex

For the reversible reaction, in the free system, the reaction process of A and B is reversible (Figure 2E). Taking the hybridization of the parallel-stranded duplex as an example, in the free system, parallel-stranded C1 and C2 hybridized and separated in equilibrium.[12] The readout of the hybridization of the parallel-stranded duplex was realized by the Thioflavin T (ThT) molecular rotor, which led to the enhanced fluorescence emission by binding into the pocket between G•G and A•A base pairs[13] (Figure S14).

As shown in Figure S15, the equilibrium between hybridization and separation of parallel-stranded duplex was influenced by the concentration of C1 and C2. For instance, C1 and C2 tended to hybridize at a concentration of 1 μM, while they tended to separate at the lower concentration of 20 nM (Figure S15 and accompanying discussion). Under such concentration conditions (20 nM), the i-motif nanostructure was applied to control the hybridization of the parallel-stranded duplex. To this end, the C1-C and C2-C (20 nM, i-motif modified strands) were designed to contain both the sequences of the i-motif and C1 and C2 (Table S5). In acidic medium, C1-C and C2-C hybridized as the

assembly of the i-tmotif, and then separated as the disassemble of i-motif in basic medium (Figure 2F and Figure S16). The results revealed that the parallel hybridization was controlled and regulated by the assembly of the pH-responsive i-motif nanostructure (Figure S17). In other words, the hybridization of C1 and C2 was enhanced at acidic pH as a consequence of the formation of the i-motif between the C traits of the C1-C and C2-C sequences. Besides such a pH-responsive i-motif nanostructure, the 2D-W DODA nanostructure was applied to regulate the parallel hybridization independent of the pH values (Figure 2G and H).

To evaluate the 2D-W DODA as an effective regulation platform, several essential control experiments were performed. Firstly, the fluorescence of ThT itself was not affected by the pH (Figure S18). Secondly, the nanostructure of 2D-W DODA stayed stable under different pH (Figure S19). Moreover, DODA itself (without C1-C or C2-C) only exhibited the background fluorescence, confirming that the ThT bound slightly with DODA (Figure S20). The results in Figure 2H and S21 revealed the DODA nanostructure favored the formation of a stable parallel-stranded duplex under different pH conditions. Comparing the i-motif and DODA systems, they both provide impetus and platforms for parallel hybridization, enhancing the formation of a parallel-stranded duplex at low concentration. Moreover, under basic conditions, the hybridized parallel-stranded duplex in the DODA system stayed stable, whereas the i-motif disassembled. Additionally, the 2D-W DODA was confirmed by FRET experiments, which further support the hybridization of C1-C and C2-C in DODA. The strand C1-C was modified by FAM, and the strand C2-C was modified by BHQ1. The FRET signal (FAM was quenched by BHQ1) was generated upon their hybridization in the DODA nanostructure (see Figure S22 and accompanying discussion).

DODA Regulated Assembly of Binary DNAzyme

For the "Inert" reaction, A and B cannot assemble into C in the free system (Figure 2I). Taking the assembly of binary DNAzyme (assembly of DZa, DZb and Helper strand) as an example, DZa, DZb and Helper strand cannot assemble into DNAzyme or cleave the substrate in the free system (Figure 2J). The native 15 % PAGE analysis demonstrated the inert assembly of DNAzyme even at the high concentration of 1 μM in the free system (Figure S24A). It is mainly caused by the weak and unstable complementary base pairings between DZa and Helper strand (9 base pairs), DZb and Helper strand (11 base pairs). The steric hindrance between the DZa and DZb could further separate them apart (Figure S24B). By programming the DZa and DZb in the DODA via the addition of Helper strand, the DNAzyme could assemble effectively, following cleaving the substrate (Figure 2K). Note that the Helper strand played a vital role in assembling the DNAzyme. The DNAzyme could not assemble without the Helper strand (Figure S25). The FRET signals verified the formation of DNAzyme in the DODA nanostructure (Figure S26). The enhanced fluorescence illustrated the cleavage of the substrate, further confirming the successful assembly of DNAzyme in the DODA nanostructure (Figure 2L, red and black curve). In order to further confirm the cleavage activities of the formed DNAzymes, the fluorescence intensity at 488 nm versus cleavage time from 0 to 24 h was plotted (Figure S27).

The Effects of Biomolecular Arrays on Their Functionalities in Four DODAs with Different Conformations

The confinement of molecular reactions within certain environments has been regarded as a decisive aspect to regulate chemical activity in space.[14] It is known that nanoconfinement can increase the stability of biomolecules such as proteins,[15] G-quadruplexes and i-motifs.[16] It is also of importance to investigate the reactivity of biomolecules in nanoconfinement. Previous works have also explored the effects of enzyme colocalization in simple geometries such as 1D, 2D scaffolds and 3D format.

Next, four DODAs with different conformations (Figure S29), hosting the same number of reactants for both A and B, were designed to explore the effects of biomolecular arrays on their functionality. As shown in Figure 3A, reactants A and B were spatially organized on the DODA nanostructures. Ten reactants A and ten B were programmed on 2D-W DODA, 2D-N DODA, 3D-W DODA and 3D-N DODA. After activation, ten products C were colocalized on a 1D array (Figure 3B and Figure S30A), a 2D array (Figure 3B and Figure S30B), a 3D-W array

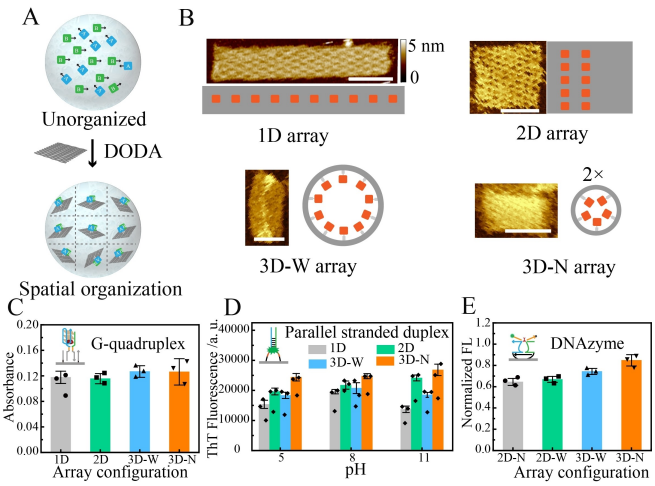

Figure 3. The effects of biomolecular arrays on their functionalities in four DODAs with different conformations. A) Organization and strategically positioning reactants A and B in DODA. B) Products C assembled by ten units were arranged in different array configurations, e.g., 1D array, 2D array, 3D-wide (3D-W) array, and 3D-narrow (3D-N) array. C) Comparisons of the catalytic activities of formed G-quadruplexes with different array configurations in different DODAs. D) Comparisons of the hybridization degree of parallel-stranded duplex with different array configurations in the four DODAs. E) Comparisons of the catalytic activities of formed DNAzymes with different array configurations in the four DODAs. Scale bars: 100 nm.

(Figure 3B and Figure S30C) and a 3D-N array (Figure 3B and Figure S30D), respectively. The results in Figure 3C, D and E indicated that the catalytic activities of G-quadruplexes, hybridization of parallel strand and catalytic cleavage performance of DNAzymes kept high catalytic activities in different arrays. No statistically significant difference was observed in different arrays. The parallel hybridization of C1-C and C2-C and catalytic cleavage performance of DNAzymes improved slightly in such crowded nanoconfinement environments (Figure 3D). More interestingly, the catalytic cleavage performance of DNAzymes was enhanced to some extent in the 3D-N DODA (Figure 3E).

Dynamical Control of Molecular Reactions with the Transformation of DODAs

Recently, the exploitations of conformational transformation of nanostructures from 2D to 3D have led to the fabrication of stimuli-responsive nanodevice systems in the targeted transport of molecular payloads,[17] cancer immunotherapy[4a,18] and many other applications. Benefiting from the tunable and controllable transformation of the DODAs from 2D-N to 2D-W, then to 3D-N, and finally to 3D-W, the molecular reactions could further be dynamically controlled and regulated. The dynamic transformation process and mechanism of DODAs from 2D-N DODA to 2D-W DODA, then to 3D-N DODA, and finally to 3D-W DODA are illustrated in Figure S1 and Figure S2 and the transformation results are supplied in Figures S31–S35. As shown in Figure 4A and Figure S36, reactants A and B were positioned spatially in 2D-N DODA, in which the A and B were spatially isolated at a distance of about 17.7 nm. Then the transformation of DODAs from 2D-N to 2D-W brought A and B into closer proximity to accomplish the assembly reactions into C effectively in 2D-W DODA. Moreover, the transformation of DODAs from 2D-W to 3D-N provided a crowded environment for product C. Finally, the transformation of DODAs from 3D-N to 3D-W moved A and B apart, resulting in the disassemble of product C (Figure 4B). Dynamic control over the assembly of a G-quadruplex has been exemplified for the first time (Figure S37). The formation of the G-quadruplex was regulated among the conformation changes of DODAs. Specifically, the G-quadruplex didn't form when Blocked-G1 and Blocked-G2 were positioned in the 2D-N DODA at a distance of around 17.7 nm. Two reasons were considered: 1) the distances between G2-block and Track 2, G1-block and Track 1 were too far for the strand displacement reaction and the G2 and G1 could not be activated. 2) Although the G2 and G1 were activated by adding the Track 2 and Track 1 extra before transformation, the distance between activated G1 and G2 was so far that they could not assemble into the G-quadruplex (Figure S38). Transformation of the DODA (from 2D-N to 2D-W) brought the G2-block and Track 2, G1-block and Track 1 into a closer proximity for strand displacement reactions, activating the G1 and G2. The activated G1 and G2 were in close proximity to assemble into the G-quadruplex. The conformational change that triggered the formation of the G-quadruplex was also confirmed by FRET. The FRET signal (Atto 488 was quenched by BHQ1) generated upon the formation of G-quadruplexes after conformational transforming from 2D-N DODA to 2D-W DODA. (Figure S39). Afterwards, when

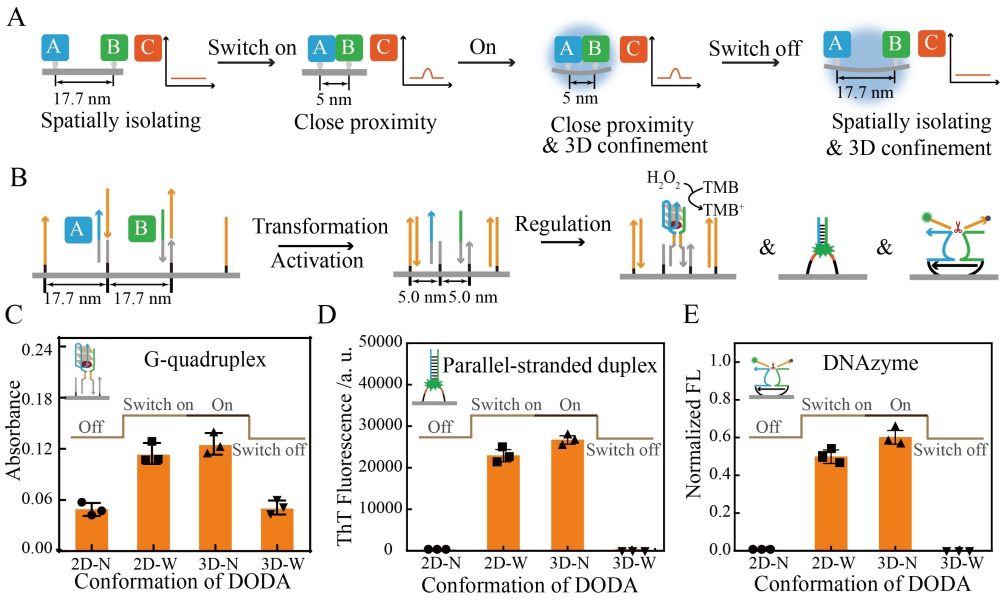

Figure 4. Dynamic control of molecular reactions with the transformation of DODAs. A) Molecular reactions were dynamically controlled and regulated by the transformation of DODAs from 2D-N to 2D-W, then to 3D-N, finally to 3D-W conformations. B) Schematic presentation of dynamic assembly of G-quadruplex, DNAzyme and parallel hybridization by the transformation of DODAs. C) The formation and catalytic activities of G-quadruplex were regulated by the transformation of the DODAs. D) The hybridization of parallel strands was regulated by the transformation of the DODAs. E) The assembly and catalytic cleavage activities of DNAzymes were regulated by the transformation of the DODAs.

the DODA's conformation transformed from 2D-W to 3D-N, the formed G-quadruplexes were maintained with active catalytic performance. Finally, when the DODA's conformation transformed from 3D-N to 3D-W, the formed G-quadruplex disassembled due to the separating of G1 and G2. To sum up, the formation of G-quadruplexes and their catalytic performance were switched between "Off—Switch on—On—Switch Off" states as the DODA's conformation transformed (Figure 4C). Similar to a G-quadruplex, the dynamic control over the hybridization of a parallel-stranded duplex was also demonstrated (Figure S40) which further verified the controllable hybridization (Figure 4D). Meanwhile, the assembly and RNA-cleaving activity of the DNAzymes were fully controlled by the transformation of DODAs (Figure 4E, Figure S41–S45). It is worth noting that the dynamic regulation process could not directly switch from the "Off" state to the "On" state without the intermediate "Switch on" state, as the consequence of the direct transformation of 2D-N to 3D-N in DODA nanostructure was prohibited.

Spatiotemporal Control of Molecular Cascade Reactions by a Reconfigurable DODA

Self-assembly of biocatalysts and the spatial control over the localization/proximity of the biocatalytic components on nanostructures have provided insight into probing numerous biocatalytic cascades in nanoconfined environments.[19] Herein, biocatalyst's assembling units A1, B1, A2 and B2 were spatially separated in 2D-N DODA. After the conformation transformation, A1 and B1 self-assembled into biocatalyst C1, A2 and B2 self-assembled into biocatalyst C2. C1 and C2 then underwent reaction cascades. In the cascade system, the substrate S1 reacted with C1, producing intermediate product P1. Then P1 acted as the substrate S2 to react with C2, resulting in the final product P2[20] (Figure 5A). As shown in Figure 5B, taking the reaction cascade between DNAzyme and G-quadruplex as an example, the DNAzymes formed after the DODA's conformation transformation from 2D-N to 2D-W. In the meantime, G1 and G2 were still blocked and the G-quadruplexes did not form yet in 2D-W DODA. After adding the C-G1$_{\text{-release}}$ (CG1r) and C-G2$_{\text{-release}}$ (CG2r), they were cleaved by the formed DNAzymes to produce intermediate products L-G1$_{\text{-release}}$ (LG1r) and L-G2$_{\text{-release}}$ (LG2r). The intermediate products LG1r and LG2r then activated the Blocked-G1 and Blocked-G2 into activated G1 and G2, resulting in the formation of G-quadruplexes. The readout of the cascade reactions was realized by observing the absorbance of 650 nm which originated from the oxidized TMB^+ by the formed hemin/G-quadruple. To induce the cascade reaction, the CG1r and CG2r were synthesized in advance. LG1r and LG2r were firstly cyclized as CG1r and CG2r, the CG1r and CG2r were then cleaved by the DNAzyme to produce LG1r and LG2r (Figure S47).

Followed by the time-dependent fluorescence changes on cleavage of the fluorophore/quencher-functionalized substrates of CG1r and CG2r that correspond to the respective DNAzyme reporter units in 2D-W DODA (Figure 5C), and the time-dependent absorbance changes of the TMB^+ generated by the formed G-quadruplex, the cascade

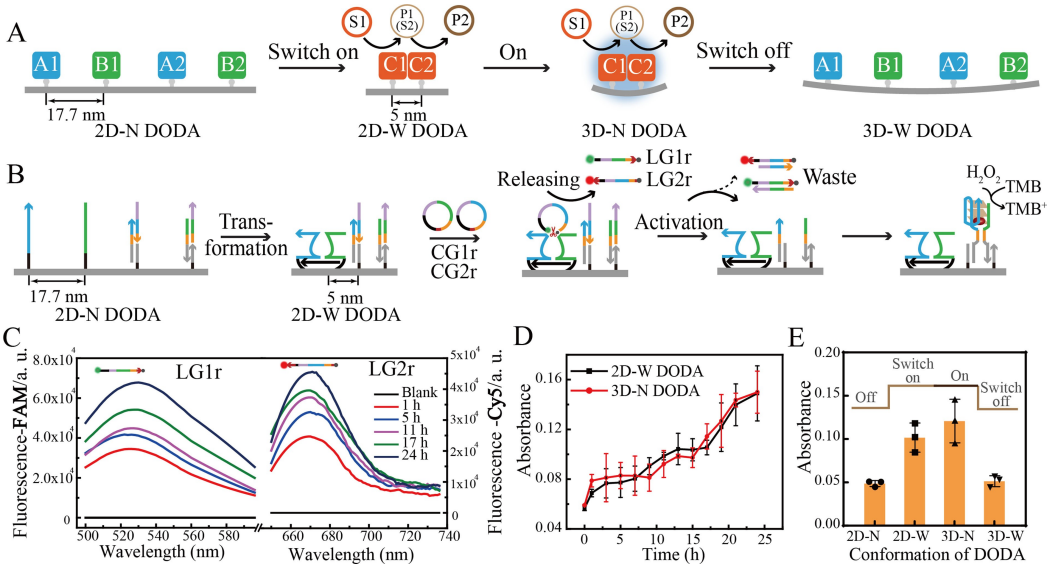

Figure 5. Molecular cascade reactions in reconfigurable DODA. A) Reaction cascades were dynamically controlled and regulated by the transformation of DODAs. S1 and P1 represent substrate and product of C1, respectively; S2 and P2 represent substrate and product of C2, respectively. B) Detailed reaction cascades between DNAzyme and G-quadruplex in reconfigurable DODA. C) Fluorescence spectra of the cleaved intermediate products LG1r (left) and LG2r (right) by the assembled DNAzymes in 2D-W DODA. D) Comparison of production of the TMB^+ product from the DNAzyme-G-quadruplex cascade reaction in 2D-W DODA and 3D-N DODA. Error bars stand for the calculated standard deviation from a set of three experimental repeats. E) Production of the TMB^+ product from the DNAzyme-G-quadruplex cascade reaction was dynamically regulated via the transformations of DODA.

reaction between DNAzyme and G-quadruplex was demonstrated (Figure 5D). Note that, the circular DNA of CG1r and CG2r were utilized to induce the cascade reaction instead of the linear ones, as the linear ones turn to form the G-quadruplex before DNAzyme cleavage and lead to a failed reaction cascade. While the circular ones could not induce the formation of a G-quadruplex before cleaving by DNAzyme (Figure S48). The reaction cascade between DNAzyme and G-quadruplex was reconfigured by the conformation transformation of DODAs (Figure 5E and S49).

Conclusion

Our work has demonstrated a reconfigurable DODA-based system to spatiotemporally control and regulate molecular cascade reactions. As a proof-of-principle, assembly of G-quadruplex, hybridization of parallel-stranded duplex and assembly of binary DNAzyme are exemplified. In the free system, the reactants were in a random configuration that prohibited dynamic and switchable control over interactions. Such DODA-based systems enable effective assembly reactions by avoiding reaction byproducts, allowing for directing the reversible assembly and activating the inert assembly. For the assembly of a G-quadruplex ("side" reaction), compared to the free system, the DODA-based system regulated the formation of the G-quadruplex specifically by G1 and G2, preventing the byproducts assembled by two G2 monomers. For the hybridization of a parallel-stranded duplex, the DODA-based system favored the hybridization of a parallel-stranded duplex, stabilizing the formed parallel-stranded duplex. For the assembly of a binary DNAzyme, DODA nanostructures provided platforms for stabilizing the base pairing between DZa and Helper strand, DZb and Helper strand, facilitating the formation of DNAzyme. The conformational transformation of DODAs from 2D-N to 2D-W, then to 3D-N and finally to 3D-W dynamically controlled and regulated three types of molecular reactions. The assembly occurs in a spatiotemporally proximal manner that could add an extra level of control to the formation of complex dynamic structures. To this end, the innovation in our approach lies in the spatial separation of assembly monomers, preventing the monomers from reacting non-specifically until triggered. Except for the involved assembly monomers, functional molecules (such as aptamers, fluorescent, therapeutic structures, proteins) can also be incorporated in DODA with high precision and structural control. Therefore, the investigation of the conformational transformation triggered cascade reactions in DODAs provided complex dynamic model systems for mimicking the natural processes and introduced the fundamental concepts to the field of systems chemistry.

Acknowledgements

We are grateful for the financial support from the National Natural Science Foundation of China (Nos. 81822024 and 22161132008), the Natural Science Foundation of Shanghai, China (Nos. 19520714100, 19ZR1475800), the Project of Shanghai Jiao Tong University (2019QYA03 and YG2017ZD07), the Starry Night Science Fund of Zhejiang University Shanghai Institute for Advanced Study (SN-ZJU-SIAS-006) and the startup funding from Institute of Basic Medicine and Cancer (IBMC), Chinese Academy of Sciences. We acknowledge the AFM characterization supported by Zhiyuan Innovative Research Center, SJTU. Special appreciation is given to Dr. Yujie Xie for proofreading of the manuscript.

Conflict of Interest

The authors declare no conflict of interest.

Data Availability Statement

The data that support the findings of this study are available in the Supporting Information of this article.

Keywords: cascade reactions · dynamic regulation · reconfigurable DNA origami · spatial control

[1] R. J. Williams, A. M. Smith, R. Collins, N. Hodson, A. K. Das, R. V. Ulijn, *Nat. Nanotechnol.* **2009**, *4*, 19–24.

[2] a) G. M. Whitesides, M. Boncheva, *Proc. Natl. Acad. Sci. USA* **2002**, *99*, 4769–4774; b) P. Jonkheijm, P. van der Schoot, A. P. H. J. Schenning, E. W. Meijer, *Science* **2006**, *313*, 80–83.

[3] a) R. Wang, C. Nuckolls, S. J. Wind, *Angew. Chem. Int. Ed.* **2012**, *51*, 11325–11327; *Angew. Chem. Int. Ed.* **2012**, *124*, 11487–11489; b) A. P. Eskelinen, A. Kuzyk, T. K. Kaltiaisenaho, M. Y. Timmermans, A. G. Nasibulin, E. I. Kauppinen, P. Torma, *Small* **2011**, *7*, 746–750; c) A. Kuzyk, R. Schreiber, Z. Fan, G. Pardatscher, E.-M. Roller, A. Hogele, F. C. Simmel, A. O. Govorov, T. Liedl, *Nature* **2012**, *483*, 311–314; d) X. Liu, F. Zhang, X. Jing, M. Pan, P. Liu, W. Li, B. Zhu, J. Li, H. Chen, L. Wang, J. Lin, Y. Liu, D. Zhao, H. Yan, C. Fan, *Nature* **2018**, *559*, 593–598; e) H. Yan, S. H. Park, G. Finkelstein, J. H. Reif, T. H. Labean, *Science* **2003**, *301*, 1882–1884; f) S. Fan, D. Wang, J. Cheng, Y. Liu, T. Luo, D. Cui, Y. Ke, J. Song, *Angew. Chem. Int. Ed.* **2020**, *59*, 12991–12997; *Angew. Chem. Int. Ed.* **2020**, *132*, 13091–13097.

[4] a) S. Liu, Q. Jiang, X. Zhao, R. Zhao, Y. Wang, Y. Wang, J. Liu, Y. Shang, S. Zhao, T. Wu, Y. Zhang, G. Nie, B. Ding, *Nat. Mater.* **2021**, *20*, 431–433; b) P. Zhang, X. Liu, P. Liu, F. Wang, H. Ariyama, T. Ando, J. Lin, L. Wang, J. Hu, B. Li, C. Fan, *Nat. Commun.* **2020**, *11*, 3114; c) S. Fan, J. Cheng, Y. Liu, D. Wang, T. Luo, B. Dai, C. Zhang, D. Cui, Y. Ke, J. Song, *J. Am. Chem. Soc.* **2020**, *142*, 14566–14573; d) L. Sun, Y. Gao, Y. Xu, J. Chao, H. Liu, L. Wang, D. Li, C. Fan, *J. Am. Chem. Soc.* **2017**, *139*, 17525–17532; e) G. Grossi, M. D. E. Jepsen, J. Kjems, E. S. Andersen, *Nat. Commun.* **2017**, *8*, 992; f) J. Song, J.-M. Arbona, Z. Zhang, L. Liu, E. Xie, J. Elezgaray, J.-P. Aime, K. V. Gothelf, F. Besenbacher, M. Dong, *J. Am. Chem. Soc.* **2012**, *134*, 9844–9847.

[5] N. V. Voigt, T. Torring, A. Rotaru, M. F. Jacobsen, J. B. Ravnsbaek, R. Subramani, W. Mamdouh, J. Kjems, A. Mokhir, F. Besenbacher, K. V. Gothelf, *Nat. Nanotechnol.* **2010**, *5*, 200–203.

[6] B. Rosier, A. J. Markvoort, B. Gumi Audenis, J. A. L. Roodhuizen, A. den Hamer, L. Brunsveld, T. F. A. de Greef, *Nat. Catal.* **2020**, *3*, 295–306.
[7] a) O. I. Wilner, Y. Weizmann, R. Gill, O. Lioubashevski, R. Freeman, I. Willner, *Nat. Nanotechnol.* **2009**, *4*, 249–254; b) J. Fu, Y. R. Yang, A. Johnson-Buck, M. Liu, Y. Liu, N. G. Walter, N. W. Woodbury, H. Yan, *Nat. Nanotechnol.* **2014**, *9*, 531–536.
[8] a) Y. Zhang, V. Pan, X. Li, X. Yang, H. Li, P. Wang, Y. Ke, *Small* **2019**, *15*, 1900228; b) S. S. Fan, D. F. Wang, A. Kenaan, J. Cheng, D. X. Cui, J. Song, *Small* **2019**, *15*, 1805554; c) D. Wang, L. Yu, B. Ji, S. Chang, J. Song, Y. Ke, *Nano Lett.* **2020**, *20*, 8236–8241; d) Y. Liu, J. Cheng, S. Fan, H. Ge, T. Luo, L. Tang, B. Ji, C. Zhang, D. Cui, Y. Ke, J. Song, *Angew. Chem. Int. Ed.* **2020**, *59*, 23277–23282; *Angew. Chem. Int. Ed.* **2020**, *132*, 23477–23482.
[9] a) A. J. Thubagere, W. Li, R. F. Johnson, Z. Chen, S. Doroudi, Y. L. Lee, G. Izatt, S. Wittman, N. Srinivas, D. Woods, E. Winfree, L. Qian, *Science* **2017**, *357*, eaan6558; b) J. Chao, J. B. Wang, F. Wang, X. Ouyang, E. Kopperger, H. J. Liu, Q. Li, J. Y. Shi, L. H. Wang, J. Hu, L. H. Wang, W. Huang, F. C. Simmel, C. H. Fan, *Nat. Mater.* **2019**, *18*, 273–279; c) S. F. J. Wickham, M. Endo, Y. Katsuda, K. Hidaka, J. Bath, H. Sugiyama, A. J. Turberfield, *Nat. Nanotechnol.* **2011**, *6*, 166–169.
[10] Y. He, D. R. Liu, *Nat. Nanotechnol.* **2010**, *5*, 778–782.
[11] J. Song, Z. Li, P. F. Wang, T. Meyer, C. D. Mao, Y. G. Ke, *Science* **2017**, *357*, eaan3377.
[12] G. A. T. C. Otto, K. Rippe, T. M. Jovin, W. L. Peticolas, *Biochemistry* **1991**, *30*, 3062–3069.
[13] a) S. Liu, P. Peng, H. Wang, L. Shi, T. Li, *Nucleic Acids Res.* **2017**, *45*, 12080–12089; b) L. Shi, P. Peng, J. Zheng, Q. Wang, Z. Tian, H. Wang, T. Li, *Nucleic Acids Res.* **2020**, *48*, 1681–1690.
[14] a) Y. Tian, J. R. Lhermitte, L. Bai, T. Vo, H. L. Xin, H. Li, R. Li, M. Fukuto, K. G. Yager, J. S. Kahn, Y. Xiong, B. Minevich, S. K. Kumar, O. Gang, *Nat. Mater.* **2020**, *19*, 789–796; b) A. Samanta, V. Sabatino, T. R. Ward, A. Walther, *Nat. Nanotechnol.* **2020**, *15*, 914–921.
[15] a) A. Brinker, G. Pfeifer, M. J. Kerner, D. J. Naylor, F. U. Hartl, M. Hayer-Hartl, *Cell* **2001**, *107*, 223–233; b) F. Takagi, N. Koga, S. Takada, *Proc. Natl. Acad. Sci. USA* **2003**, *100*, 11367–11372.
[16] a) P. Shrestha, S. Jonchhe, T. Emura, K. Hidaka, M. Endo, H. Sugiyama, H. Mao, *Nat. Nanotechnol.* **2017**, *12*, 582–588; b) S. Jonchhe, S. Pandey, T. Emura, K. Hidaka, M. A. Hossain, P. Shrestha, H. Sugiyama, M. Endo, H. Mao, *Proc. Natl. Acad. Sci. USA* **2018**, *115*, 9539–9544.
[17] S. M. Douglas, I. Bachelet, G. M. Church, *Science* **2012**, *335*, 831–834.
[18] S. Li, Q. Jiang, S. Liu, Y. Zhang, Y. Tian, C. Song, J. Wang, Y. Zou, G. J. Anderson, J. Y. Han, Y. Chang, Y. Liu, C. Zhang, L. Chen, G. Zhou, G. Nie, H. Yan, B. Ding, Y. Zhao, *Nat. Biotechnol.* **2018**, *36*, 258–264.
[19] M. Vázquez-González, C. Wang, I. Willner, *Nat. Catal.* **2020**, *3*, 256–273.
[20] M. Levy, A. D. Ellington, *Proc. Natl. Acad. Sci. USA* **2003**, *100*, 6416–6421.

Manuscript received: November 30, 2021
Accepted manuscript online: December 21, 2021
Version of record online: January 11, 2022